ELSEVIER

Polymer 43 (2002) 6813–6819

polymer

www.elsevier.com/locate/polymer

The effect of filler type, morphology and coating on the anisotropy and microstructure heterogeneity of injection-moulded discs of polypropylene filled with aluminium and magnesium hydroxides. Part 2. Thermal and dynamic mechanical properties

J.I. Velasco[a,*], C. Morhain[a], A.B. Martínez[a], M.A. Rodríguez-Pérez[b], J.A. de Saja[b]

[a]*Centre Català del Plàstic, Universitat Politècnica de Catalunya, C. Colom 114 Terrassa, Barcelona 08222, Spain*
[b]*Departamento de Física de la Materia Condensada, Cristalografía y Mineralogía, Facultad de Ciencias, Universidad de Valladolid, Prado de la Magdalena s/n, 47011 Valladolid, Spain*

Received 25 March 2002; received in revised form 30 May 2002; accepted 13 September 2002

Abstract

Thermal and dynamic mechanical characteristics of injection-moulded discs of polypropylene (PP) filled with 40% by weight of magnesium and aluminium hydroxides have been studied by means of differential scanning calorimetry and dynamic mechanical thermal analysis, and have been related to the anisotropy and microstructure heterogeneity of the discs. The effect of filler type, particle morphology and surface coating has been analysed. The nucleation activity of filler particles on PP has been quantified and found to be reduced in coated grades of magnesium hydroxide. The employed coatings worked isolating and preserving particles surface from direct interaction with polymer chains. The different orientations of both filler particles and PP α crystals were found to be the main cause of the differences observed in mechanical properties.

Keywords: Polypropylene; Flame retardant fillers; Injection-moulding

1. Introduction

Mineral fillers can reduce the production costs of polypropylene moulded parts, increase the material stiffness and heat deflection temperature (HDT), reduce the shrinkage of the moulded parts and also can increase the tensile strength and fracture toughness depending mainly on particle morphology and surface coating [1–6].

Aluminium and magnesium hydroxides are increasingly being incorporated in PP due to its flame-retardancy and smoke-suppressing effect [7]. In spite of mechanical properties deterioration [8,9] the benefits offered by these fillers, in particular flame retardancy, are achieved for high filler contents [10,11].

In injection-moulded parts of filled PP, both polymer phases and anisometric filler particles remain highly oriented. The inner structure of the part is far from being homogeneous or isotropic [12,13] and it is dependent on the moulding conditions.

PP crystalline phases in mineral filled composites can also display anisotropic properties. Recent investigations on these topics in talc-filled PP composites have proved that certain filler surface treatments based on silane coupling agents promote higher anisotropy in injection-moulded discs than untreated talc [14,15]. Furthermore, a critical value of filler concentration of 20 wt% has been found in uncoated magnesium hydroxide filled PP composites [16], for which the polymer crystal anisotropy degree shows a maximum value. In this case, the PP crystal orientation is strongly induced by that of the $Mg(OH)_2$ particles.

Following these investigations, in the present work we have prepared a series of filled PP composites with aluminium and magnesium hydroxides, having similar filler loading (40 wt%), to study the effect of the filler type, particle morphology and surface coating on the anisotropy and heterogeneity of injection-moulded discs. The establishment of the samples microstructure, based on wide-angle X-ray diffraction (WAXD) measures, was the first part

* Corresponding author. Tel.: +34-937837022; fax: +34-937841827.
E-mail address: jose.ignacio.velasco@upc.es (J.I. Velasco).

0032-3861/02/$ - see front matter
PII: S0032-3861(02)00669-9

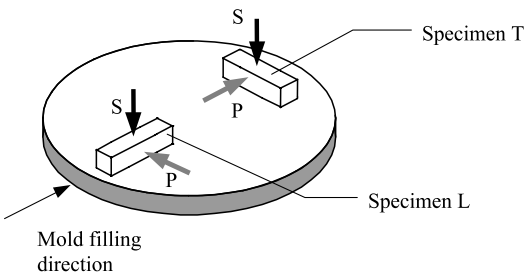

Fig. 1. Specimens and testing directions in the injection-moulded discs.

of the work, and it is shown as a separate publication [17]. The present paper shows the second part, consisting of thermal and dynamic mechanical characterisation of the composites.

2. Materials, compounding and specimens

The basic characteristics of polymer and fillers, as well as the compounding and injection-moulding procedures are detailed in Ref. [17].

Prismatic bars (25 mm × 4 mm × 4 mm) were machined from the injection-moulded discs to use them as testing specimens to characterise the heterogeneity and anisotropy. As shown in Fig. 1, 'L' specimens were cut from the zone of the disc closer to the mould cavity gate, having its length axis parallel to the main flow direction. 'T' specimens were cut from the opposite zone of the disc with its length axis perpendicular to the main flow direction.

3. Experimental

3.1. Melt flow index and heat deflection temperature

To have information about the influence of the fillers on the molten-state characteristics of the filled polymer, measures of the melt flow index (MFI) and the volumetric melt flow index (MFI-v) were taken at 190 °C and 2160 g of load.

Values of the HDT were obtained at a heating rate of 2 °C/min applying a three-point-bending stress of 1.8 MPa on injection-moulded prismatic specimens of nominal dimensions 127 × 12.7 × 6.35 mm^3. The selected span was 100 mm.

3.2. Differential scanning calorimetry (DSC)

A *Mettler* DSC-30 thermal analysis system was employed for thermal characterisation. The temperature was calibrated by using indium, zinc and lead. Energy was calibrated by using an indium reference sample. To study the nucleation activity of the fillers in the PP crystallisation behaviour, each sample was first heated at 200 °C for 4 min to erase the thermal history. The measurements were carried out from 200 to 10 °C at the following cooling rates: 2, 5, 10, 20 and 40 °C/min. After each cooling experiment a heating experiment between 10 and 200 °C was performed. Samples weighing about 5 mg were used. The crystallinity of PP and the nucleation activity of the filler were calculated. The crystallinity was calculated with the equation:

$$X_c = \frac{\Delta H_m m_c / m_p}{\Delta H_0} \quad (1)$$

Where ΔH_m is the melting enthalpy measured in the heating experiments, ΔH_0 is the theoretical value of enthalpy of 100% crystalline PP ($\Delta H_0 = 207.1$ J/g) [18], m_c is the mass of the sample, and m_p is the mass of PP in the sample.

The non-isothermal crystallisation process was studied following the method developed by Dobreva and Gutzow [19,20] for the study of the crystallisation kinetics of polymer melts in presence of inorganic substrates [21]. The relationship proposed by these authors is the following

$$\log q = \text{const} - \frac{B}{2.3\Delta T^2} \quad (2)$$

where q is the crystallisation rate, ΔT the undercooling ($T_m - T_p$) with T_m the melting temperature and T_p the crystallisation temperature of the sample. The activity of nucleation of the filler is related to the parameter ϕ

$$\phi = \frac{B^*}{B^0} \quad (3)$$

Where B^* is the value of B when the polymer is filled with the nucleant agent, and B^0 when it is unfilled. From the experimental slopes in the plots $\log q$ versus $1/\Delta T^2$ it is possible to obtain the B values and, by using Eq. (3), the parameter ϕ can be estimated. The nucleation activity of the filler is related to this parameter (ϕ) so that a lower value of ϕ deals with a higher activity. Previous works have shown that this parameter is very useful to analyse the effect of fillers on the crystallisation kinetics and consequently on the properties of filled polymers [15,16,21].

From the definition of B, the polymer crystal surface energy (σ) can be estimated:

$$B = \frac{16\pi\sigma^3 V_m^2}{3kT_m\Delta S_m^2 n} \quad (4)$$

And finally the lamella thickness (L), from the variant of the Gibbs–Thomson equation for a crystal of large lateral dimensions and finite thickness [22,23]:

$$T_m = T_m^0\left[1 - \frac{2\sigma_e}{L\Delta H_m}\right] \quad (5)$$

In the above equations, k is the Boltzman's constant, T_m the PP melting temperature, ΔH_m the PP melting enthalpy and σ_e the specific surface energy. The polypropylene molar volume (V_m) was taken equal to 28 cm^3 mol^{-1}, the molar entropy (ΔS_m) 24.2 J K^{-1} mol^{-1}, the Avrami exponent $n = 3$ and the melting temperature at equilibrium (T_m^0) 479 K [24,25].

Table 1
PP crystalline characteristics determined by DSC

Sample	Melting temperature,[a] T_m (K)	Crystallinity,[a] X_c (%)	Activity parameter, ϕ	Surface energy, σ (10^{-6} J cm^{-2})	Lamella thickness (nm)
PP	437.3	47.7	1	2.028	5.18
PPH5	437.2	51.3	0.765	1.855	4.39
PPH5L	437.3	48.4	0.873	1.939	4.89
PPHKV	437.2	49.1	0.840	1.913	4.73
PPOL	437.9	53.3	0.563	1.676	3.89
PPON	438.1	51.0	0.571	1.684	4.10

[a] Average value from the five endothermic melting signals recorded by heating at 10°/min, after cooling at 2, 5, 10, 20 and 40 °C/min.

3.3. Dynamic mechanical thermal analysis (DMTA)

DMTA testing was performed using a Perkin–Elmer DMTA 7. The testing configuration was three-point bending (20 mm span). A static stress of 6 MPa and a dynamic stress of ± 5 MPa with a frequency of 1 Hz were applied.

Tests were performed in two perpendicular directions for each sample. As shown in Fig. 1, in *S* configuration the specimen surfaces that support the load correspond to the surfaces of the moulded disc. However, in *P* configuration the load is applied on the perpendicular surfaces. For each specimen (L and T) and for each direction (*S* and *P*) two kinds of tests were performed. On one hand, dynamic loading was isothermally applied (at 20 °C) on the samples in order to get quantitative results. The values of the storage modulus (E') and the loss tangent (tan δ) were measured 5 min after applying the stresses, i.e. once the initial fluctuations of the values had disappeared. On the other hand, the characterisation of the glass transition was carried out through tests performed in the range of temperature from −40 to 40 °C, at a heating rate of 5 °C/min. Some previous experiments were done with lower heating rates (1 and 0.04 °C/min) to test the independence of the results with thermal inertia.

The glass transition temperature (T_g) was determined as the temperature corresponding to the maximum value of the loss modulus. In addition, the intensity of the transition (S_I) was quantified by using [26]

$$S_I = \frac{E'_b - E'_a}{E'_a} \quad (6)$$

Where E'_b and E'_a are, respectively, the storage modulus values before (at −20 °C) and after the transition (at the temperature of the inflexion point after the maximum in the tan δ curve). This parameter gives an estimation of the amount of amorphous phase and its mobility; the higher the value of S_I the higher the content and/or mobility of the amorphous phase are.

4. Results and discussion

4.1. Thermal properties

From the DSC non-isothermal crystallisation tests values of the nucleation activity parameter ϕ were computed (Table 1). The nucleation rate of the PP phase increased as follows: PP < 40H5L < 40H5KV < 40H5 < 40ON ≤ 40 OL. Therefore, on the one hand, $Al(OH)_3$ presented higher nucleation activity than $Mg(OH)_2$ for PP, and on the other hand, the effect of the examined surface treatments was a reduction of the nucleation activity. As a consequence of the preceding result, the crystallinity of the PP phase increased, and the surface energy and lamella thickness decreased following the same previously given trend (Fig. 2). Therefore, it is feasible to infer that the interactions between the PP phase and the $Al(OH)_3$ particles surface are stronger than those between the PP and the $Mg(OH)_2$ particles. A possible reason for this behaviour would be connected to the similar Bravais lattice of PP and $Al(OH)_3$, both monoclinic. However, $Mg(OH)_2$ crystallises in a different system; the hexagonal lattice. In the case of filler particles being capable of supporting epitaxial polymer crystallisation on their surfaces, such crystallisation is considered to require the ionic spacing of the filler crystal lattice to be close to the crystallographic dimensions of the polymer crystal [27].

In aluminium hydroxide filled samples the lower particle size of OL grade with respect of that ON seemed to slightly promote the immobilisation of polypropylene molecules. Moreover, the surface treatments used in $Mg(OH)_2$ decreased the immobilisation degree of the polypropylene in comparison with the non-treated case. Both coatings would work isolating and preserving the particle surface

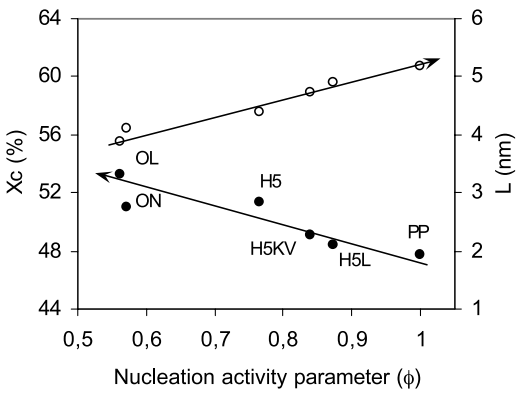

Fig. 2. Crystallinity (X_c) and lamella thickness (L) as a function of the nucleation activity parameter (ϕ).

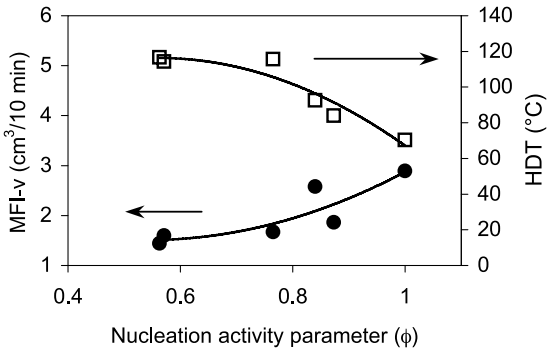

Fig. 3. MFI-v and HDT as a function of the activity parameter (ϕ).

from direct interactions with the PP molecules. Consequently, a lower nucleation rate would be expected.

PP molecule movement restriction caused by the different fillers has also been detected in the molten state through the MFI-v values. It is well known that the presence of mineral fillers into polymers induces a degree of molecule immobilisation on the particle surface, this fact affecting both the molten-state properties, i.e. increasing the material viscosity, and the solid-state ones (i.e. increasing elastic modulus, tensile strength, HDT, etc.). These changes could be a consequence of the development of an interface formed by immobilised molecules on the particle surface, and/or due to the development of fine and homogeneous crystalline texture formed as a result of a fast nucleation process. The amount and intensity of the polymer immobilisation depends on several factors such as, the filler Bravais lattice, the filler surface energy, its morphology, etc. As shown in Fig. 3, a growing trend is displayed when values of the MFI-v are plotted as a function of the parameter ϕ. This result suggests that a relationship between the nucleation rate and the melt viscosity exist. In this sense, the two surface treatments applied to the $Mg(OH)_2$ particles, H5L and H5KV showed a clear lubricant effect, reducing the MFI-v values. Furthermore, a contrary effect appears when the HDT values are plotted as a function of the parameter ϕ.

To summarise, in mineral filled PP samples, as higher filler/polymer interactions, higher molecule immobilisation and, as a consequence, higher melt viscosity and higher nucleation rate. Due to this, higher crystallinity and finer crystalline texture, and as a result of this, higher deformation temperature (higher HDT values).

4.2. Dynamic mechanical properties

The dynamic mechanical properties have been summarised in Table 2 for all the materials, specimens and testing directions.

4.2.1. Storage modulus

The storage modulus of all the materials, measured at 20 °C in different directions, is displayed in Fig. 4. As expected, the storage modulus resulted higher for the composites than for the PP, this result can be easily understood taking into account firstly the higher stiffness of the particles, and secondly the higher orientation degree of the polymer in the composites. In this sense, Fig. 5 shows the storage modulus as a function of the PP phase orientation characterised by the WAXD ratio $I(040)/I(110)$. The graphic suggests that the main source for the

Table 2
Dynamic-mechanical characteristics

Sample		E'^{a} (GPa)	tan δ^{a}	$T_g{}^{b}$ (°C)	$S_I{}^{b}$
PP	LS	1.10	0.053	0.0	0.90
	LP	0.76	0.049	−2.0	1.08
	TS	0.93	0.050	0.6	0.63
	TP	0.75	0.051	−0.6	1.16
PPH5	LS	2.08	0.035	1.2	0.49
	LP	1.34	0.057	−1.2	0.82
	TS	1.88	0.026	0.8	0.51
	TP	1.27	0.062	−2.2	0.76
PPH5L	LS	1.76	0.040	1.2	0.55
	LP	1.03	0.066	−1.0	0.83
	TS	1.53	0.048	1.0	0.62
	TP	1.05	0.072	−1.2	0.68
PPH5KV	LS	1.67	0.026	−0.4	0.57
	LP	1.05	0.065	−3.0	0.82
	TS	1.55	0.030	0.6	0.53
	TP	1.06	0.078	−1.4	0.55
PPOL	LS	1.90	0.038	0.6	0.53
	LP	1.10	0.062	−2.2	0.82
	TS	1.75	0.037	−0.2	0.48
	TP	1.09	0.055	−2.0	0.67
PPON	LS	1.72	0.039	1.2	0.70
	LP	0.95	0.064	−4.2	0.74
	TS	1.69	0.039	0.6	0.61
	TP	1.02	0.056	−1.6	0.82

[a] Values determined from tests performed isothermally at 20 °C.
[b] Values determined from tests performed at a heating rate of 5 °C/min in the range between −20 and 40 °C.

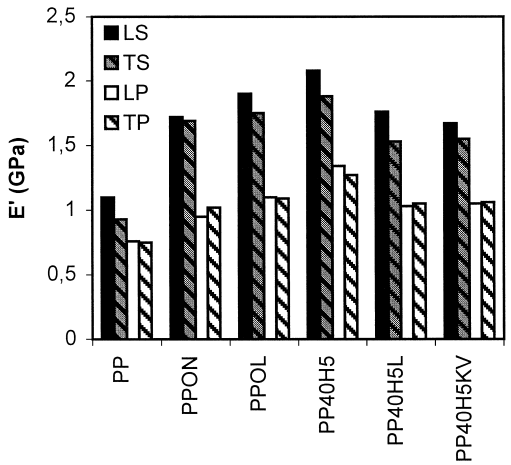

Fig. 4. Storage modulus at room temperature for all the materials, specimens and directions studied.

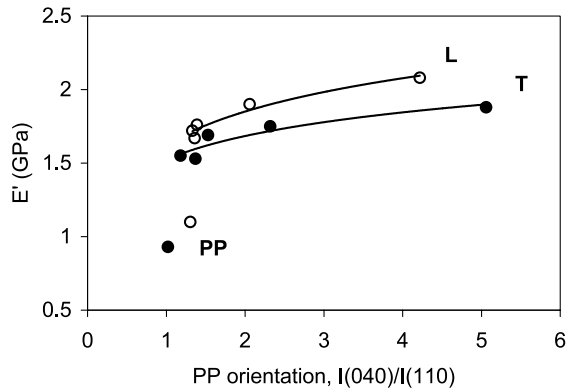

Fig. 5. Storage modulus at room temperature measured in the *S* direction as a function of the PP crystal orientation from WAXD measures (orientation data taken from Ref. [17]).

differences between the modulus of the different composites could be the different orientation of the PP phase.

If the materials filled with untreated fillers are considered, it can be observed that PPH5 has the highest modulus, consequently it can be deduced that the magnesium hydroxide particles have a stronger effect on the composite stiffness than the aluminium hydroxide ones. Another interesting result is inferred when values of materials with surface-treated fillers are observed; the treatments used for $Mg(OH)_2$ particle surface clearly reduce the stiffness of the filled materials.

The storage modulus resulted higher when the tests were performed under *S* configuration, especially for filled samples. This result is another evidence of the strong mechanical anisotropy of the tested samples. The skin and core contribution to the mechanical behaviour is very different if the applied stress is parallel or pependicular to the specimen surface. On the one hand, the maximum stresses are mainly applied to the samples skin under *S* test configuration. On the other hand, as it was shown by WAXD, the inorganic particles were placed mainly parallel to the surface of the mould in the sample skin and the PP orientation was maximum in this zone. Both reasons allow explaining the higher modulus obtained under *S* configuration. When the experiments are performed applying the stress parallel to the *P* direction the skin does not play the same important role because the maximum stresses are applied mainly to the disc core.

The samples heterogeneity can be analysed by inspection of the differences of modulus between L and T specimens. Under *S* configuration the L samples result stiffer. This should be explained in terms of the different skin thickness in the specimens. It is well known that the skin thickness progressively decreases in injection-moulded parts from zones near to the gate to zones far away from it. The thicker skin could account for the higher modulus of the L samples when loaded in *S* configuration. On the other side, the storage modulus measured in *P* direction results similar for L and T samples. Under this configuration the main contribution to the stiffness comes from the specimens core,

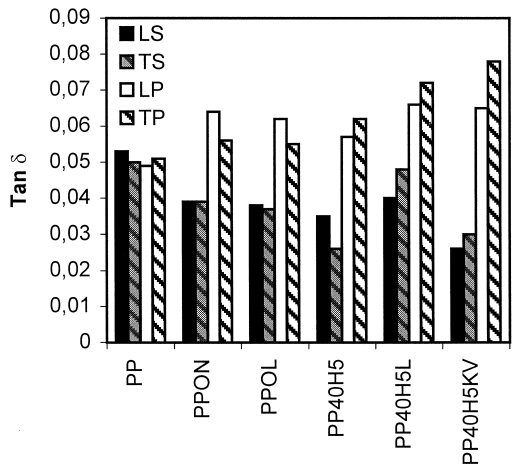

Fig. 6. Loss tangent at room temperature for all the materials, specimens and directions under study.

what presents a similar orientation of both filler particle and PP crystalline phase for L and T samples.

4.2.2. Loss tangent

The obtained values of the loss tangent show different trends if the data for *S* and *P* directions are examined (Fig. 6).

As it was previously pointed out, under *S* configuration, the skin specimen contribution is decisive. The polymer and the particles present a high degree of orientation in this zone. These two characteristics imply high storage modulus and low values of the loss factor. As a consequence, similar trends for the storage modulus as a function of the kind of filler used and its treatment can also be observed when the tan δ values are considered. On the other hand, there is no a clear trend for the differences between the tan δ of the L and T samples.

4.2.3. Glass transition

No significant differences between the values of the glass transition were detected (Table 2). This result seems to indicate that the degree of interaction between the particles and the PP was not strong enough to modify the temperature of activation of molecular movements.

4.2.4. Transition intensity

The comparison of the transition intensity values between L and T samples (Fig. 7(a)) is quite interesting because provides attractive information about the polymer phase heterogeneity. In general, L samples present higher S_I values than the T ones, the explanation of this result should be related to the different amorphous content of both specimens. L samples present a thicker skin, i.e. a higher content of polymer that was cooled very quickly from the melt. Because of that should present a higher amorphous content. It is interesting to remark that there are different trends for the S_I parameter for different materials. Firstly, unfilled PP has the highest S_I values and shows the greatest

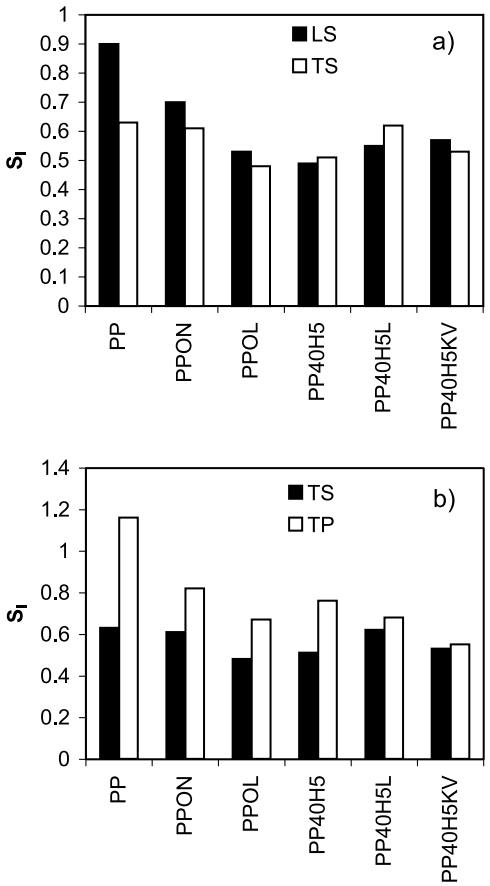

Fig. 7. (a) Glass transition intensity measured under *S* configuration. (b) Glass transition intensity for T samples.

differences between L and T specimens. Secondly, the ON composite has lower values and lower L–T differences than the unfilled PP. Finally, the OL material and the PP/magnesium hydroxide composites have the lowest values and the lowest differences.

The differences of the transition intensity between the samples measured under *S* and *P* configuration are shown in Fig. 7(b). The values are clearly higher in the *P* direction due to the reduced molecular mobility of the PP in the skin.

5. Conclusions

Both kinds of mineral particles were found to act as nucleating agents for polypropylene crystallinity. Nevertheless, aluminium hydroxide particles displayed a higher nucleation effect than magnesium hydroxide ones. This result could be explained due to similar Bravais lattice of this mineral and that of polypropylene α crystal. No effect of $Al(OH)_3$ particle morphology was observed on the nucleation activity. However, particle surface coatings notably reduced the nucleation activity of magnesium hydroxide. These surface treatments seemed to work isolating and preserving the particle surface from direct interaction with polypropylene chains. In fact, they displayed lubricant effect for PP in the molten state.

The injection-moulded discs analysed were quite anisotropic and heterogeneous from a point of view of dynamic mechanical behaviour. By one hand, different characteristics were observed depending on the measurement direction. As expected, the samples were stiffer when the load was applied under *S* configuration. This could be explained due to different orientations of both filler particles and polymer crystals in the specimen skin respect to the core. The main role for the difference of the storage modulus between the composites seemed to be the PP orientation in the skin zone. Furthermore, no differences between the glass transition temperature of PP in the different composites were detected.

By the other hand, the heterogeneity of the discs was also characterised in terms of dynamic mechanical properties. All the filled materials presented a similar degree of heterogeneity, although the storage modulus was found to be higher for L samples than for T ones.

Acknowledgements

The authors thank to MCYT (Government of Spain) for the financial assistance of the project MAT 2000-1112. Also, C. Morhain thanks to CIRIT (Government of Catalonia, Spain) the concession of a predoctoral grant.

References

[1] Pukánszky B. In: Karger-Kocsis J, editor. Particulate filled polypropylene: structure and properties. Polypropylene: structure, blends and composites, vol. 3. London: Chapman & Hall; 1995. p. 1–70.
[2] Stricker F, Bruch M, Mulhaupt R. Polymer 1997;38:5347–53.
[3] Vollenberg PHT, Heikens D. Polymer 1989;30:1656–62.
[4] Velasco JI, de Saja JA, Martínez AB. Fatigue Fract Engng Mater Struct 1997;20:659–70.
[5] Velasco JI, Morhain C, Arencón D, Santana OO, Maspoch ML. Polym Bull 1998;41:615–22.
[6] Velasco JI, Morhain C, Maspoch ML, Santana OO. In: Brown MW, de los Rios ER, Miller KJ, editors. Effect of particle size on the fracture behaviour of aluminium hydroxide filled polypropylene. Fracture from defects, vol. 3. Cradley Heath: EMAS; 1998. p. 1381–6.
[7] Troitzsch J. Fire retardant plastics. International plastics flammability handbook. Munich: Hanser; 1990. p. 43–62.
[8] Jancar J, Kucera J. J Mater Sci 1981;26:4878–82.
[9] Velasco JI, Morhain C, Arencón D, Maspoch ML. Macromol Symp 2001;169:165–70.
[10] Velasco JI, Maspoch ML, Morhain C. Información Tecnológica 1998; 9(3):219–22.
[11] Hornsby PR, Rothon RN. Polym Degrad Stab 1996;54:383–5.
[12] Fujiyama M, Wakino T. J Appl Polym Sci 1991;42:2739–47.
[13] Fujiyama M. Int Polym Process 1992;7:165–71.
[14] Díez-Gutiérrez S, Rodríguez-Pérez MA, de Saja JA, Velasco JI. Polymer 1999;40:5345–53.
[15] Díez-Gutiérrez S, Rodríguez-Pérez MA, de Saja JA, Velasco JI. J Appl Polym Sci 2000;77:1275–83.

[16] Velasco JI, Morhain C, Martínez AB, Rodríguez-Pérez MA, de Saja JA. Macromol Mater Engng 2001;286:719–30.
[17] Velasco JI, Morhain C, Martínez AB, Rodríguez-Pérez MA, de Saja JA. Polymer 2002;43:6805–11.
[18] Wunderlich B. Thermal analysis. New York: Academic Press; 1990. p. 418.
[19] Dobreva A, Gutzow IJ. Non-Cryst Solids 1993;162:1–12.
[20] Dobreva A, Gutzow IJ. Non-Cryst Solids 1993;162:13–25.
[21] Rodríguez-Pérez MA, Vasiliev TS, Dobreva-Veleva A, de Saja JA, Gutzow I, Velasco JI. Macromol Symp 2001;169:137–42.
[22] Lauritzen Jr. JI, Hoffman JD. J Res Natl Bur Stand 1960;64A:73–102.
[23] Hoffman JD, Lauritzen Jr. JI. J Res Natl Bur Stand 1961;65A: 297–336.
[24] Varga J. J Mater Sci 1992;27:2557–79.
[25] Velasco JI, de Saja JA, Martínez AB. J Appl Polym Sci 1996;61: 125–32.
[26] Jancar J. J Mater Sci 1991;26:4123–9.
[27] Hooks DE, Fritz T, Ward MD. Adv Mater 2001;13:227–41.